Catalyst Attrition in Fluidized-Bed Systems

J. Werther and J. Reppenhagen
Technical University Hamburg-Harburg, D-21071 Hamburg, Germany

Catalyst attrition has often been a major obstacle in the development of new fluidized-bed processes and it is still of concern for existing processes whenever the catalyst is changed. The main consequence of attrition is the generation of fines and the resulting loss of valuable material. In this work the attrition of FCC catalysts in a fluidized-bed system consisting of a bubbling bed, cyclone gas cleaning, and external solids recirculation is studied. An approach developed describes the attrition-induced overall solids loss based on the main attrition sources: grid jet attrition, bubble-induced attrition, and attrition in the cyclone. Their respective contributions to the overall attrition rate are calculated from separately derived model equations that take into account the design of the system, the operating conditions, and the material properties of the catalysts. The solids entrainment from the bed into the cyclone is shown to have a strong effect on the attrition-induced loss rate and must therefore be taken into account for an a-priori prediction.

Introduction

Efficient gas–solid contacting, good bed-to-wall heat transfer, and excellent temperature homogeneity are well-known characteristics of fluidized-bed reactors. These beneficial properties are all related to the mobility of the particles in the fluidized state. But the particle motion also causes a major drawback, namely catalyst attrition due to interparticle collisions and bed-to-wall impacts. Catalyst attrition has often been a major obstacle in the development of new fluidized-bed processes and is still of concern for existing processes whenever the catalyst is changed.

The main consequence of attrition is the generation of fines, which are finally passing through the dust recovery system, resulting in a loss of valuable material. In addition to the entailed costs some authors (such as Kraft et al., 1956; de Vries et al., 1972; Pell and Jordan, 1988) report on a second drawback of the loss of fines, namely that the considered bed particle-size distribution gets too coarse. In practice, the addition of fresh makeup catalyst is therefore necessary to keep the system at a required level of fines. An opposite effect, however, may occur when the attrition-produced fines are kept inside the system. The bed particle-size distribution may then get too fine (such as Braca and Fried, 1956).

A lot of work has been done in the field of catalyst attrition. The majority of it deals with the catalysts' degradation in standardized attrition tests, as, for example, submerged jet tests (such as Forsythe and Hertwig, 1949; Gwyn, 1969), or Grace-Davison jet-cup tests (such as Weeks and Dumbill, 1990). These tests are primarily intended to rank different candidate catalysts with respect to their propensity to attrition. But they cannot predict the quantitative extent of attrition that will occur with the tested materials in a fluidized-bed process. They cannot even guarantee that the ratio of the attrition rates of two catalysts will be the same in the test and in the process. The main reason for this limited applicability is that the prevailing stress mechanism in a test differs from that prevailing in the process.

A quantitative prediction of the attrition effect in a given process requires a detailed understanding of the basic attrition mechanisms. Unfortunately, there is still a lack of physically sound explanations for the observed attrition phenomena. This has been demonstrated by Ghadiri et al. (1992), who revealed strong discrepancies in the previously published literature with respect to the influence of the superficial gas velocity on the attrition-induced loss rate of a fluidized-bed system. Some workers (such as Seville et al., 1992) relate their experimental results to $(u - u_{mf})$, others assume the attrition rate to be proportional to u^n, where the exponent varies from $n = 1$ (Patel et al., 1986) to $n = 5.8$ (Blinichev et al., 1968). The strong differences in the experimental findings are attributed to strong differences in the systems and the solids that have been considered.

In a systematic investigation of the attrition phenomena the particular effects of solids and system must be taken into account. One key point is the distinction between the differ-

Correspondence concerning this article should be addressed to J. Werther.
Present address of J. Reppenhagen: BMH Claudius Peters AG, Schanzenstrasse 40, D-21614 Buxtehude, Germany.

ent attrition modes (Pell, 1990). The mode of attrition may vary from pure abrasion to a total fragmentation of the particles. Abrasion implies that exclusively asperities are removed from the particle surface. It thus produces a lot of elutriable fines, whereas the particle-size distribution of the mother particles is hardly changed. In contrast to this, fragmentation is a process of particle breakage into similarly sized pieces. There are various attrition modes that can be regarded as somehow lying in between these two extremes, as, for example, the surface fragmentation of catalyst particles that was observed by Reppenhagen and Werther (1998a). All of these modes are based on different mechanisms and must therefore be investigated separately.

The second key point for a systematic investigation of the attrition phenomena in fluidized-bed systems is a distinction between the different regions, which apply different mechanical stress to the solids (such as Vaux and Keairns, 1980). A first approach to find these individual sources of attrition was made by Zenz (1971) and Zenz and Kelleher (1980). They revealed the necessity of studying each of these sources in isolation in order to get detailed information about the respective attrition mechanisms. They suggested investigating the vicinity of a multihole gas distributor, the bubbling fluidized bed, the cyclones, the conveying lines, and solids feeding devices as separate regions where the attrition mechanisms are different.

In the present work the attrition of FCC catalysts in a cold-model fluidized-bed system with external solids recirculation is considered. An approach is developed that describes the attrition-induced overall solids loss rate on the basis of the main attrition sources. The corresponding individual attrition rates are calculated from separately derived model equations that take into account the design of the system, the operating conditions and the material properties of the catalysts. Furthermore, the solids transport from the bed into the cyclone is found to have a strong effect on the attrition-induced loss rate and must therefore be taken into account for an *a priori* modeling.

Theory

With respect to the attrition-induced loss rate a fluidized bed with external solids recirculation appears as shown in Figure 1. Three regions can be identified as main attrition sources, namely the grid jets, the bubbling bed itself, and the cyclone section. With respect to the latter source the extent of attrition is affected by the solids transport in the freeboard. The entrainment determines the solids flow into the cyclone and thus the amount and the particle-size distribution of the material that is subjected to attrition in the cyclone.

Catalyst particles are often produced in spray-drying processes. When such a catalyst is used in an industrial fluidized-bed process the weak agglomerates may in an initial phase undergo fragmentation. But after this first phase the particles will be abraded rather than broken unless a critical mechanical stress is exceeded. Since the respective threshold is usually beyond the stress that is prevailing in a fluidized-bed reactor (cf. Reppenhagen and Werther, 1998b), the present work deals with pure abrasion only. Based on this idea the following approach is made.

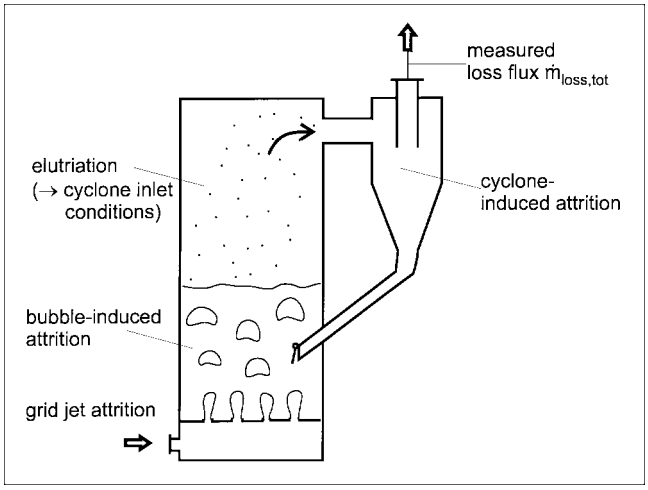

Figure 1. Relevant mechanisms with respect to the attrition-induced loss rate of the fluidized-bed system.

Since the abrasion-produced fines are rather small, that is, typically smaller than about 1 to 3 microns, the respective grade efficiency of the cyclones is distinctly smaller than unity. Therefore, it can be assumed that the fines are immediately lost after their production, even if they are produced in the jetting region or in the bubbling bed. In contrast to this, it can be assumed that after an initial phase where the original elutriable material is sifted off, the mother particles are entirely kept inside the system. Due to the mode of pure abrasion, the change in their particle size is negligible, as is their contribution to the loss rate. Hence, some kind of steady state can be assumed where the production of fines, which originate from the almost unchanged mother particles, is balanced by the loss rate of fines. The resulting quasi-stationary loss rate can therefore be written as the sum of the fines generation in the individual attrition sources

$$\dot{m}_{\mathrm{loss,tot}} = \dot{m}_{\mathrm{loss},j} + \dot{m}_{\mathrm{loss},b} + \dot{m}_{\mathrm{loss},c} \tag{1}$$

where $\dot{m}_{\mathrm{loss},j}$, $\dot{m}_{\mathrm{loss},b}$ and $\dot{m}_{\mathrm{loss},c}$ are the masses of elutriable fines that are produced per unit time by attrition in the jetting region, the bubbling bed, and the cyclone, respectively. With this division of the total loss rate the different mechanisms that contribute to the abrasion-induced loss rate are explained. They must be described individually before they are again combined in an overall description of the total process. A modeling of the individual attrition sources requires their prior investigation in isolation. For the particular attrition sources that are considered in the present work, this has already been done in previous work of the authors.

Grid jet attrition has been studied by Werther and Xi (1993) on the basis of a comprehensive experimental program. Considering the energy utilization of the abrasion process they derived the following relationship for the grid-induced attrition rate:

$$\dot{m}_{\mathrm{loss},j} = n_{\mathrm{or}} \cdot K_j \cdot \rho_f \cdot d_{\mathrm{or}}^2 \cdot u_{\mathrm{or}}^3, \tag{2}$$

where n_{or} is the number of orifices in the distributor, ρ_f is

the density of the jet gas, d_{or} is the diameter of the orifices, u_{or} is the jet gas velocity inside an orifice, and K_j is a constant that characterizes the solids' susceptibility to abrasion. Xi (1993) has shown that this constant again can be divided into a product of the surface mean diameter d_{pb} of the bed solids and a particle-size independent material-specific constant C_j, that is, the solids susceptibility to abrasion increases linearly with its surface mean diameter

$$K_j = C_j \cdot d_{pb}. \tag{3}$$

For a consideration of the overall process in the fluidized bed the orifice velocity can be substituted by the superficial gas velocity

$$u_{or} = u \cdot \frac{D_t^2}{n_{or} \cdot d_{or}^2}, \tag{4}$$

where D_t is the diameter of the fluidized-bed column. With Eqs. 3 and 4, Eq. 2 can finally be transformed to

$$\dot{m}_{loss,j} = C_j \cdot d_{pb} \cdot \rho_f \cdot \frac{D_t^6}{d_{or}^4 \cdot n_{or}^2} \cdot u^3. \tag{5}$$

More recently, Reppenhagen and Werther (1998a,b,c) investigated the abrasion-induced fines production in the cyclone. Considering again the energy utilization of the abrasion process, they derived the following model equation for cyclones, which was found to be valid for all cyclones with a tangential inlet, regardless of size and geometry

$$\dot{m}_{loss,c} = \dot{m}_{c,in} \cdot C_c \cdot d_{pc} \cdot \frac{u_{c,in}^2}{\sqrt{\mu_c}}. \tag{6}$$

In Eq. 6 $\dot{m}_{c,in}$ is the solids mass flow rate entering the cyclone, d_{pc} is the respective surface mean diameter, $u_{c,in}$ is the gas velocity at the cyclone inlet, and μ_c is the solids loading, which is defined as

$$\mu_c = \frac{\dot{m}_{c,in}}{\dot{m}_f} = \frac{\dot{m}_{c,in}}{\rho_f \cdot u_{c,in} \cdot A_{c,in}}, \tag{7}$$

where $A_{c,in}$ is the cross-sectional area of the cyclone inlet. In Eq. 6, C_c is again a particle-size independent constant that characterizes the material's attritability. For a consideration of the overall process the cyclone inlet velocity can be substituted by an expression of the superficial gas velocity

$$u_{c,in} = u \cdot \frac{A_t}{A_{c,in}}. \tag{8}$$

In the case of several equal-sized cyclones arranged in parallel, $A_{c,in}$ is the sum of their inlet areas. With Eqs. 7 and 8, Eq. 6 can now be written as

$$\dot{m}_{loss,c} = C_c \cdot d_{pc} \cdot \sqrt{\dot{m}_{c,in}} \cdot \sqrt{\rho_f} \cdot \frac{A_t^{2.5}}{A_{c,in}^2} \cdot u^{2.5}. \tag{9}$$

The mechanisms of bubble-induced attrition are not quite clear (Werther and Reppenhagen, 1999). There are various theoretical and empirical approaches that can be summarized as

$$\dot{m}_{loss,b} = K_b \cdot m_b^n \cdot (u - u_{min}), \tag{10}$$

where m_b is the bed mass, its exponent varying between 1 and 2. In the case of $n = 1$, it is implied that the attrition stress does not change with the bed height, there being simply a linear increase with the amount of treated material. In contrast to this an exponent $n > 1$ implies an increase of the attrition stress with the bed height. The velocity u_{min} is regarded as a threshold velocity above which the bubble-induced attrition occurs. Its value varied from $u_{min} = u_{mf}$ to $u_{min} \gg u_{mf}$. Therefore, a further study of this source is required before Eq. 10 can be applied.

Hence, in Eq. 1 only the terms for jet-induced and cyclone attrition can be substituted by Eqs. 5 and 9, respectively, which leads to the following provisional expression for the total loss rate of the system

$$\dot{m}_{loss,tot} = C_j \cdot d_{pb} \cdot \rho_f \cdot \frac{D_t^6}{d_{or}^4 \cdot n_{or}^2} \cdot u^3 + \dot{m}_{loss,b} + C_c \cdot d_{pc} \cdot \sqrt{\dot{m}_{c,in}} \cdot \sqrt{\rho_f} \cdot \frac{A_t^{2.5}}{A_{c,in}^2} \cdot u^{2.5}. \tag{11}$$

Experimental Studies

Fluidized-bed system with external solids circulation

The experiments, which focused on the overall system behavior, were carried out in a cold-model fluidized-bed unit that is shown in Figure 2. It mainly consists of a cylindrical column 0.2 m in diameter and 2.1 m in height. The fluidizing

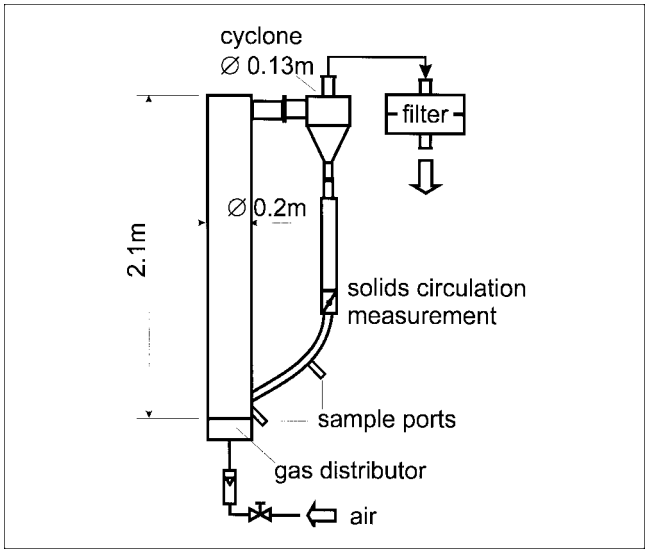

Figure 2. Experimental setup for the investigation of the attrition-induced loss rate from a fluidized-bed system.

gas is provided by a compressed-air supply at a rate up to 0.1 m^3/s. Two different types were used as a gas distributor; on the one hand, a porous plate, and on the other hand, a perforated plate with $n_{or} = 640$ orifices of $d_{or} = 0.0007$ m in diameter. In the column, the particles are held in a fluidized state by the upflowing gas stream. Some of them are entrained into the freeboard above the fluidized bed, where they are accelerated and carried upward by the gas. These particles leave the main column through an abrupt exit into the 0.13-m-ID cyclone. The rectangular cross section of the column exit is identical to that of the cyclone inlet, that is, $A_{c,in} = 1.06 \times 10^{-3}$ m^2. The particles that are separated from the gas descend in the 0.025-m-ID return line until they are finally fed back to the fluidized bed. The solids circulating rate, and with it the approximate solids mass flow into the cyclone, is measured by temporarily closing a valve in the return line and timing the mass accumulation of solids above the closed valve. The inventory of the solid particles in the lower part of the return line guarantees that steady state feeding into the bed is not interrupted during this measurement. The cyclone overflow is connected to a filter that collects the elutriated material. At steady-state attrition the quasi-stationary loss rate can then be obtained from an increase in the filter weight per unit time. Furthermore, sample ports are installed in the return line and in the fluidizing column at a height of 0.05 m above the distributor.

A fresh fluidized cracking catalyst material "97-G(fresh)" was used as bed material. In order to meet the model assumption of completely unentrainable mother-particles the original powder was screened on an 80-μm sieve prior to the experiments. The resulting particle-size distribution is shown in Figure 3. Because of the grade efficiency curve of the sieve and the irregular shape of the particles, the test material still contains particles smaller than 80 μm, that is, the particle-size distribution starts at approximately 30 μm. But from the comparison with the theoretical grade efficiency curve of the cyclone it is obvious that this minimum particle size is still coarse enough to ensure 100% collection of the mother particles. The grade efficiency curve in Figure 3 has been calculated from Trefz and Muschelknautz (1993) for the worst

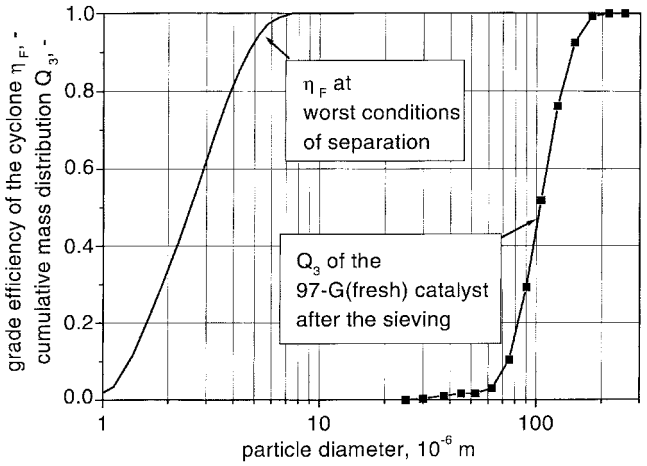

Figure 3. Particle size distribution of the test material after sieving procedure and cyclone's grade efficiency.

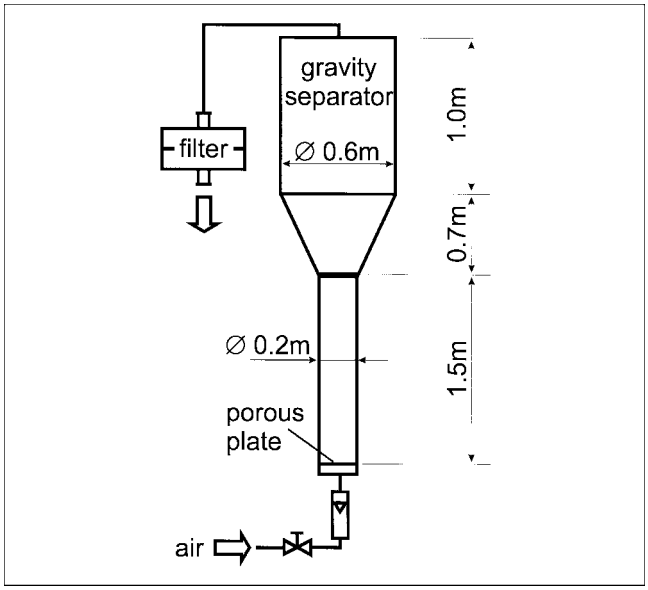

Figure 4. Test facility for the investigation of bubble-induced attrition.

separation conditions that were chosen in the course of the present work, or $u_{c,in} = 18$ m/s, $\mu_c = 0.2$. Nevertheless, it becomes unity at approximately 7.5 μm, which is distinctly smaller than the minimum particle size of 30 μm of the test material.

Bubble-induced attrition test

The material's susceptibility to bubble-induced attrition was studied in the 0.2-m-ID fluidized bed shown in Figure 4. The fluidizing gas is again provided by a compressed-air supply. In order to avoid jet attrition a porous plate is used as the gas distributor, and instead of a cyclone the column diameter is enlarged to a 0.6-m-ID gravity separator starting at a height of 1.5 m above the distributor. The loss rate of the system, which is at steady-state attrition identical to bubble-induced mass of fines produced per unit time, is determined by means of a subsequent filter.

Jet-induced attrition test/submerged jet test

A material's sensitivity against jet attrition should be investigated in a so-called submerged jet test where the bed height is higher than the jet penetration length. The maximum attrition effect of the jets is measured in such a test (cf. Werther and Xi, 1993). However, jet-induced attrition cannot be investigated in isolation, because there is always some additional attrition of the surrounding bubbling bed. In order to get direct insights into the mechanisms of jet attrition it is necessary to separate the jet contribution from the overall attrition extent.

In the present work this has been realized by using the apparatus shown in Figure 5. It consists of a 1-m-high 0.05-m-ID column with a 0.15-m-ID gravity separator on top. The mass of fines produced per unit time is again measured by means of a subsequent filter. The key point of the test apparatus is the gas distributor. A separately fed nozzle is inte-

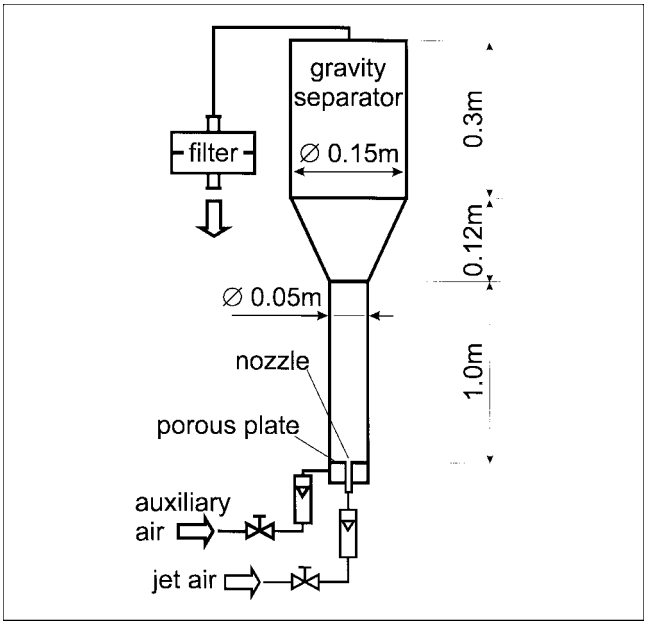

Figure 5. Test facility for the investigation of jet attrition.

grated into the center of the porous plate, which is also aerated to prefluidize the bed and to keep the bubble-induced attrition constant. In this way the bubble attrition must be determined only once even if the jet gas velocity is varied. This is conveniently done without any jet gas prior to the true experiment without any jet gas.

Cyclone attrition test

The experimental setup for evaluating the material susceptibility to cyclone attrition is shown in Figure 6. It mainly consists of a 0.09-m-ID cyclone that is operated in the suction mode. The solids are introduced via a vibrating feeder into a 0.3-m-long inlet tube. After a test run the underflow of the cyclone is used as a starting material for the next run. The cyclone loss for each pass is collected in a filter.

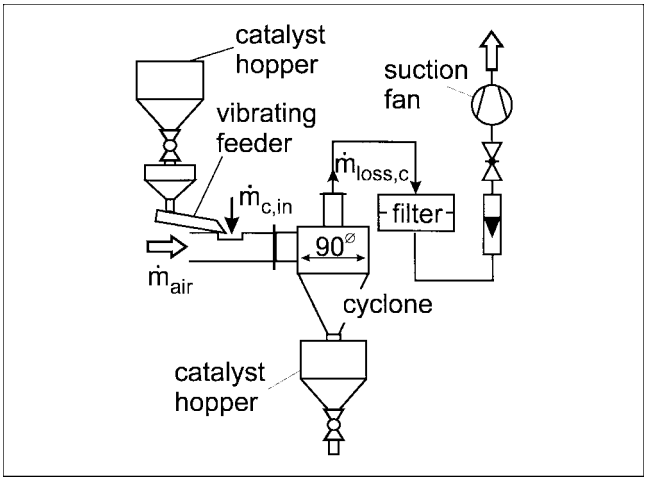

Figure 6. Experimental setup for the investigation of cyclone attrition.

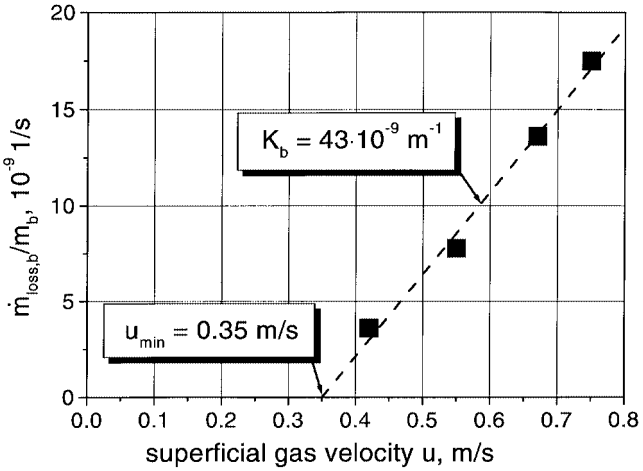

Figure 7. Results of the bubble attrition tests plotted according to Eq. 10.

Results and Discussion

Investigation of bubble-induced attrition

In order to study the mechanisms of bubble-induced attrition, the fluidized bed test apparatus shown in Figure 4 was operated with 5.75 kg of initial material at various superficial gas velocities. Figure 7 shows the results, which are plotted as a function of the gas velocity. In agreement with Eq. 10, they can be described by the product of an attrition constant $K_b = 43 \times 10^{-9}$ m^{-1}, and the difference between the superficial gas velocity and a threshold velocity $u_{\min} = 0.35$ m/s, which is distinctly larger than the minimum fluidization velocity of the material, or $u_{mf} = 0.005$ m/s. However, the measured data are also sufficiently described by the power-law dependence on the excess gas velocity. A least-squares regression yields an exponent of 2.89, which can be rounded up to 3, as is shown in Figure 8. It can thus be written

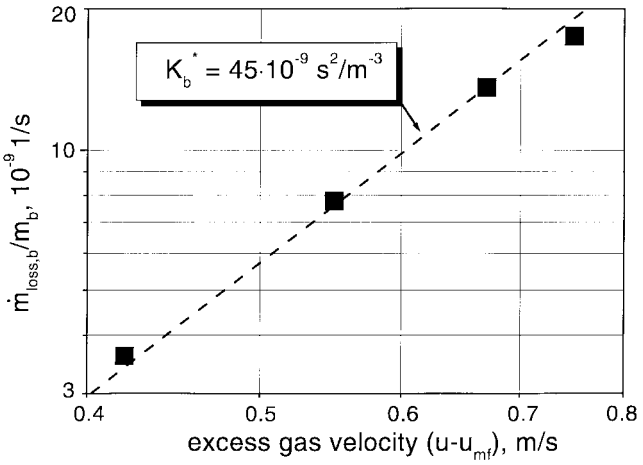

Figure 8. Results of the bubble attrition tests plotted according to Eq. 12.

$$\dot{m}_{\text{loss},b} = K_b^* \cdot m_b \cdot (u - u_{mf})^3, \qquad (12)$$

where $K_b^* = 45 \times 10^{-9}$ s^2/m^3 is again an attrition constant. Equation 12 is used in the following to describe the bubble-induced attrition in the entire fluidized-bed system. In comparison to Eq. 10, which is as empirical, it describes the measured data equally well, but requires one parameter only. It should be noted that the present work is not primarily intended to study in detail the mechanisms of bubble-induced attrition, but rather to provide a systematic procedure to identify and to summarize the relevant mechanisms of the overall attrition phenomena. For this purpose Eq. 12 may be taken as sufficient, even though it does not take into account the influence of the particular flow regime and is thus not based on physical explanations. In particular, since the fluidized-bed system shown in Figure 2 has the same bed geometry as the bubble attrition test unit, Eq. 12 can be introduced into model Eq. 11

$$\dot{m}_{\text{loss,tot}} = C_j \cdot d_{pb} \cdot \rho_f \cdot \frac{D_t^6}{d_{\text{or}}^4 \cdot n_{\text{or}}^2} \cdot u^3 + K_b^* \cdot m_b \cdot (u - u_{mf})^3 + C_c \cdot d_{pc} \cdot \sqrt{\dot{m}_{c,\text{in}}} \cdot \sqrt{\rho_f} \cdot \frac{A_t^{2.5}}{A_{c,\text{in}}^2} \cdot u^{2.5}. \qquad (13)$$

Evaluation of the material's susceptibility to cyclone attrition

In order to determine the particle-size-independent cyclone attrition rate constant C_c of the test material accurately, the previously screened initial material was further divided into various fractions of different particle size. For each fraction, cyclone attrition tests (cf. Figure 6) were carried out in order to evaluate its respective attritiability, which is expressed by the particle-size-dependent cyclone attrition constant

$$K_c = C_c \cdot d_{pc}. \qquad (14)$$

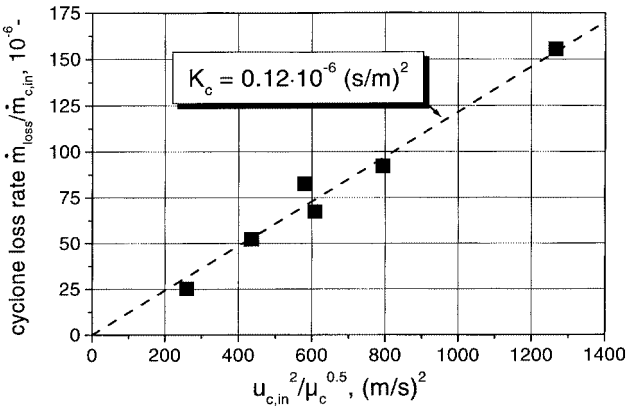

Figure 9. Particle-size-dependent cyclone attrition constant K_c for the entire material fraction on the basis of cyclone attrition tests.

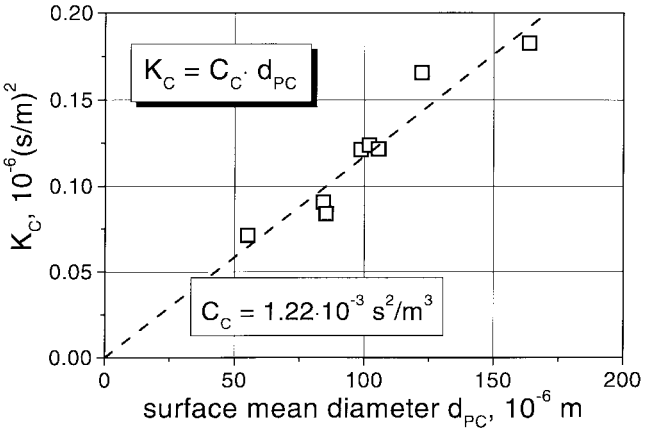

Figure 10. Particle-size-independent cyclone attrition constant C_c from the particle-size-dependent constants K_c of several individual-size fractions.

As an example, Figure 9 shows the experimental results obtained for the entire initial particle-size distribution. The material was passed through the cyclone at different operating conditions as long as the lost mass per single pass reached a constant value, that is, the quasi-stationary cyclone attrition was reached. According to Eq. 6, the respective quasi-stationary loss rates are plotted as a function of the ratio of the square of the inlet velocity to the square-root of the solids loading. The rate constant K_c is then identified as the slope of the regression line.

For the individual size fractions the respective values of K_c were obtained analogously and plotted as a function of the respective surface mean diameter (cf. Figure 10). According to Eq. 14, the particle-size-independent attrition constant is now identical to the slope of the regression line, or $C_c = 1.22 \cdot 10^{-3}$ s^{2}m^3.

Comparison of jet attrition and cyclone attrition

Before the fluidized-bed system was considered as a whole, a comparison was made between the two attrition sources that already can be described on the basis of physically sound equations, namely jet attrition by Eq. 5 and cyclone attrition by Eq. 6. For this purpose, another six FCC catalysts were subjected to both jet attrition tests and cyclone attrition tests in order to determine the respective particle-size-independent attrition rate constants C_j and C_c. The latter were obtained as in the previous section. The values for the jet attrition constants were obtained by a similar procedure: the materials were again divided into fractions with different particle sizes. Approximately 300 g of these material fractions were then subjected to jet attrition tests in the apparatus that is shown in Figure 5. In these tests both the orifice velocity u_{or} and the orifice diameter d_{or} were varied. The respective particle-size-dependent attrition constant K_c was derived from the steady-state loss rates, according to Eq. 2. The attrition constants of the various fractions were then used to obtain the particle-size-independent attrition constant C_c, as illustrated in Figure 11 for the 85-A(e-cat) catalyst.

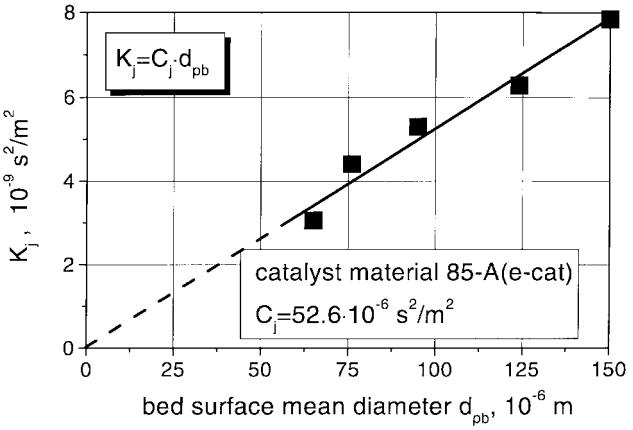

Figure 11. Particle-size-independent jet attrition constant C_j from the particle-size-dependent constants K_j of several individual-size fractions.

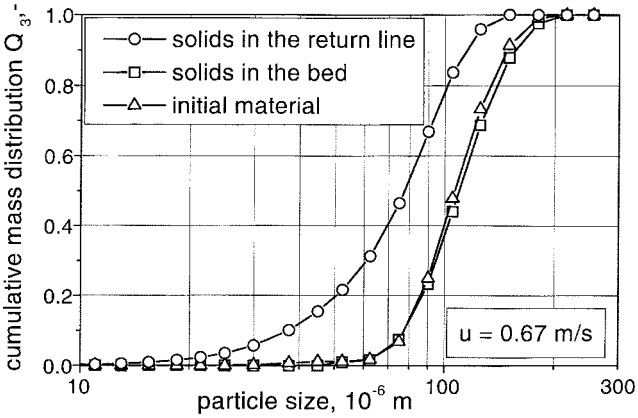

Figure 13. Influence of entrainment on local particle-size distributions in the fluidized-bed system.

Figure 12 compares the attrition rate constants for the six considered catalysts. For illustration purposes the values for C_j and C_c are related to the respective values of the most attrition-resistant catalyst type, the 97-A(e-cat). Although Figure 12 basically shows material properties only, the diagram may be regarded as a plot of attrition rates of the catalysts relative to the 97-A(e-cat), provided that the particle-size distributions and the operating conditions are kept the same. The catalysts are arranged in ascending order with respect to the value of the jet attrition. Obviously, the ranking of the catalysts would be slightly different if it was done with respect to cyclone attrition, that is, 94-K(fresh) and 85-A(e-cat) would change positions. Apart from this partly different ranking of the catalysts by the different sources, it is in any case impossible to derive the ratio of the cyclone attrition constants of two materials from the ratio of the jet attrition constants and vice versa.

The differences in the effects of the two attrition sources can be attributed to the quite different attrition mechanisms they are based on. In the case of jet-induced attrition-interparticle impacts are responsible, whereas in the case of cyclone attrition, the particle friction and particle impact on the cyclone walls can be considered to be responsible. This comparison adds further evidence to the necessity of considering and modeling the different attrition sources separately. There is no way of predicting the attrition caused by the one source on the basis of the findings for another source.

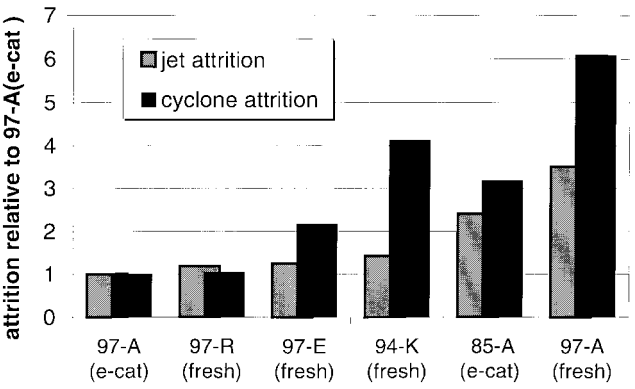

Figure 12. Jet attrition with cyclone attrition for different types of catalysts.

Local particle-size distributions in the fluidized-bed system

In the experiments with the entire fluidized-bed system, catalyst samples were taken from the bed and from the return line as soon as the system had reached the steady state, that is, a quasi-stationary loss rate was measured. Figure 13 shows the particle-size distributions of samples that were taken from an experiment with a superficial gas velocity of 0.67 m/s. From a comparison with the initial material it can be seen that the particle-size distribution in the return line is distinctly shifted to a smaller particle-size range. As a consequence, the particle-size distribution in the bed is shifted to the larger particle-size range. But the change in the particle-size distribution of the bed material is only a very slight one, and thus can be neglected in the present case.

Attrition-induced overall loss rate from a fluidized-bed system with porous plate distributor

First attrition experiments in the overall system were carried out using a porous plate as a gas distributor in the fluidized-bed system. In this particular case, only two attrition sources must be taken into account, namely the bubbling bed and the cyclone. With the previously derived information about the respective catalyst's attrition characteristics ($C_c = 1.22\times10^{-3}$ s²/m³ and $K_b^* = 45\times10^{-9}$ s²/m³), it is now possible to calculate the total attrition-induced loss rate of a system on the basis of Eq. 13 by simply omitting the term for the jet-induced attrition.

As an example, the system was operated at a superficial gas velocity of $u = 0.67$ m/s, where a total loss rate of $\dot{m}_{\text{loss, tot}} = 0.318\times10^{-6}$ kg/s was measured. The essential information about the system design and the operating conditions, including the approximate surface mean diameter of the entrained material, is summarized in the second column of Table 1. With these data the individual contributions of

Table 1. Data of the Experiments with the Fluidized-Bed System

System Geometry				
D_t, m	0.2	0.2	0.2	0.2
A_t, m^2	0.0314	0.0314	0.0314	0.0314
$A_{c,\mathrm{in}}$, m^2	1.06×10^{-3}	1.06×10^{-3}	1.06×10^{-3}	1.06×10^{-3}
Type of distributor plate	Porous	Perforated	Perforated	Perforated
n_{or}	N/A	640	640	640
d_{or}, m	N/A	0.0007	0.0007	0.0007
Operating Variables				
u, m/s	0.67	0.67	0.71	0.74
m_b,'kg	5.5	5.5	5.5	5.5
Measured Quantities				
$\dot{m}_{c,\mathrm{in}}$, 10^{-3} kg/s	2.5	2.0	2.7	4.0
d_{pc}, 10^{-6} m	62	69	71	69
d_{pb}, 10^{-6} m	105	104	107	107
$\dot{m}_{\mathrm{loss,tot}}$, 10^{-6} kg/s	0.318	0.551	0.639	0.827
Calculated Attrition Rates				
$\dot{m}_{\mathrm{loss},i}$, 10^{-6} kg/s	—	0.242	0.293	0.332
$\dot{m}_{\mathrm{loss},b}$, 10^{-6} kg/s	0.075	0.075	0.089	0.100
$\dot{m}_{\mathrm{loss},c}$, 10^{-6} kg/s	0.235	0.234	0.330	0.425
$\dot{m}_{\mathrm{loss,tot}}$, 10^{-6} kg/s	0.310	—	0.712	0.857

both the bubble-induced and the cyclone attrition can be calculated and derived for the total loss rate of the system:

$$\dot{m}_{\mathrm{loss,tot}} = K_b^* \cdot m_b \cdot (u - u_{mf})^3 + C_c \cdot d_{pc} \cdot \sqrt{\dot{m}_{c,\mathrm{in}}} \cdot \sqrt{\rho_f} \cdot \frac{A_t^{2.5}}{A_{c,\mathrm{in}}^2} \cdot u^{2.5}$$
$$= 0.075\times10^{-6}\ \mathrm{kg/s} + 0.235\times10^{-6}\ \mathrm{kg/s}$$
$$= 0.310\times10^{-6}\ \mathrm{kg/s}, \qquad (15)$$

which is very close to the measured value. According to this example, it is possible to describe the total loss rate of a fluidized-bed system as the sum of the contributions of its individual sources.

Attrition-induced overall loss rate of the fluidized-bed system with perforated-plate distributor

In order to describe the loss rates in the case of the perforated-plate distributor an additional attrition characteristic is required, namely the particle-size-independent jet attrition constant C_j. In general, this can be obtained from experiments like those described earlier. However, this additional effort is not needed now. The previous section has shown that the contribution of the other attrition sources can be described on the basis of the derived model equation. Therefore, the contribution of the jet-induced attrition, and thus the jet attrition constant, can be determined from the loss rate of the system itself. For this purpose, the system was again operated at a superficial gas velocity of $u = 67$ m/s, but using the perforated-plate distributor instead of the porous plate. The respective information about the system is given in the third column of Table 1.

As can be seen from Table 1, the measured loss rate of $\dot{m}_{\mathrm{loss,tot}} = 0.551\times10^{-6}$ kg/s is distinctly higher than the one previously measured with the porous-plate distributor. However, the difference cannot be directly assigned to the distributor attrition, because the particle-size distributions of the respective initial materials, and thus the mass flow rate and the particle-size distribution of the entrained material, were different. Consequently, the contribution of the cyclone attrition must be newly calculated by Eq. 9, which leads to $\dot{m}_{\mathrm{loss},c} = 0.234\times10^{-6}$ kg/s (*Note:* Despite the 20% decrease in the system's entrainment rate the cyclone attrition is almost identical to the previous experiment. The reason is the compensation by the 15% increase in the mean surface diameter of the entrained material.) The contribution of the jet attrition can now be calculated from the overall loss rate by subtracting the contributions of bubble-induced and cyclone attrition

$$\dot{m}_{\mathrm{loss},j} = \dot{m}_{\mathrm{loss,tot}} - \dot{m}_{\mathrm{loss},b} - \dot{m}_{\mathrm{loss},c}$$
$$= 0.551\times10^{-6}\ \mathrm{kg/s} - 0.075\times10^{-6}\ \mathrm{kg/s} - 0.234\times10^{-6}\ \mathrm{kg/s}$$
$$= 0.242\times10^{-6}\ \mathrm{kg/s}. \qquad (16)$$

The required particle-size-independent jet attrition constant C_j can now be obtained from a simple transformation of Eq. 5:

$$C_j = \dot{m}_{\mathrm{loss},j} \cdot \frac{d_{\mathrm{or}}^4 \cdot n_{\mathrm{or}}^2}{d_{pb} \cdot \rho_f \cdot D_t^6 \cdot u^3}$$
$$= 9.9\times10^{-6}\ \mathrm{s^2/m^3}. \qquad (17)$$

With the derived value of C_j the required information about the material's susceptibility to abrasion is complete. Equation 13 can now be applied to calculate the total loss rates of the fluidized-bed system at various gas velocities. This is demonstrated on the basis of two additional experiments carried out at $u = 0.71$ m/s and $u = 0.74$ m/s. Again, both the essential information for the calculation and the calculation results are summarized by Table 1. As can be seen from this table, even a slight change in the superficial gas velocity leads to a significant increase in the measured total loss rate. This phenomenon is well described by the model, Eq. 13.

Furthermore, from the respective calculations of the individual contributions of attrition sources, it is obvious that the cyclone attrition is most significantly affected by a change in the gas velocity, even though the respective attrition mechanism has the lowest sensitivity against the gas velocity, that is, $\dot{m}_{\text{loss},c} \propto u^{2.5}$ in contrast to $\dot{m}_{\text{loss},b} \propto (u - u_{mf})^3$ and $\dot{m}_{\text{loss},j} \propto u^3$. This effect can be mainly attributed to the increase in the entrainment rate, because according to Eq. 9, cyclone attrition increases with the square root of the entrained mass flow rate. However, the entrainment rate itself of the system increases with u^n, with the exponent being in the $n = 2$ to $n = 4$ range (such as Geldart, 1986). Hence, the true sensitivity of the cyclone attrition against the gas velocity is much higher in a fluidized-bed system than in an isolated configuration. It may range from $\dot{m}_{\text{loss},c} \propto u^{3.5}$ to $\dot{m}_{\text{loss},c} \propto u^{4.5}$, and this is consequently higher than the sensitivity of the other sources.

A-Priori Modeling

The model Eq. 13 requires knowledge of the mean surface diameter and the mass flow rate of the entrained material. Both values change with the operating conditions, and especially significant are the effects of changes in the mass flow rate on the cyclone attrition, as was shown in the previous section. It is, therefore, necessary to take these effects into account. This can be either done by measurements if an existing process is considered, or by an entrainment/elutriation model in the case where *a-priori* modeling of attrition is required. In general it can be written

$$\dot{m}_{c,\text{in}} = A_t \cdot G_s = A_t \cdot \sum_i G_{si} = A_t \cdot \sum_i w_i \cdot K_i^*, \tag{18}$$

where G_s is the total solids elutriation rate from the bed, G_{si} is the fractional elutriation rate for the size interval i, w_i is the weight fraction of the size interval i in the bed material, and K_i^* is the respective elutriation rate constant. There are various correlations suggested in the literature to calculate a material's elutriation rate constants. In the present work, the correlation suggested by Tasirin and Geldart (1998) is chosen, which was derived from experiments with FCC catalysts in a similarly sized fluidized-bed system

$$K_i^* = 14.5 \cdot \rho_f \cdot u^{2.5} \cdot \exp\left(-5.4 \frac{u_{ti}}{u}\right), \tag{19}$$

where u_{ti} is the terminal velocity of the size interval i. The entrained mass flow rate into the cyclone can be calculated by the insertion of Eq. 19 into Eq. 18. The respective surface mean diameter can be estimated from

$$d_{pc}(u) = \frac{G_s}{\sum_i \frac{G_{si}}{x_i}} = \frac{G_s}{\sum_i \frac{w_i \cdot K_i^*}{x_i}}, \tag{20}$$

where x_i is the mean diameter of the size interval i. With Eqs. 18, 19, and 20 the model Eq. 13 can now be written as

$$\dot{m}_{\text{loss,tot}} = C_j \cdot d_{pb} \cdot \rho_f \cdot \frac{D_t^6}{d_{\text{or}}^4 \cdot n_{\text{or}}^2} \cdot u^3 + K_b^* \cdot m_b \cdot (u - u_{mf})^3 + 3.81 \cdot C_c \cdot d_{pc}(u) \cdot \rho_f \cdot \frac{A_t^3}{A_{c,\text{in}}^2} \cdot \sqrt{\sum_i w_i \cdot \exp\left(-5.4 \frac{u_{ti}}{u}\right)} \cdot u^{3.75}. \tag{21}$$

On the basis of Eq. 21 the total loss rate and the contributions of the individual sources of a given system now can be calculated *a priori*, depending on the superficial gas velocity. Using the same values for the material's attrition rate constants and the system design as in the previous section, this is demonstrated in Figure 14, where the respective values are plotted as a function of the gas velocity. This once more illustrates the strong sensitivity of the cyclone attrition inside a fluidized-bed system to the superficial gas velocity. It is significantly higher than the sensitivities of jet- or bubble-induced attrition, respectively.

Moreover, it is obvious that due to these different dependencies the role of the main attrition source changes with the gas velocity. In the lower velocity range—in this particular example, $u < 0.55$ m/s—the gas distributor is the main attrition source, whereas at higher velocities cyclone attrition is dominant. If the loss rate of a given process must be minimized, such a consideration provides strong support for the previous cost-benefit analysis, because the measures should naturally be first applied to the main attrition source. It should be noted in this context, however, that in practice a system operating at the higher superficial gas velocities should under all circumstances be designed to avoid loss rates that fall on the steep section of the total loss curve in Figure 14. This can be achieved by designing the grid holes and the cyclone to operate at sufficiently low velocities.

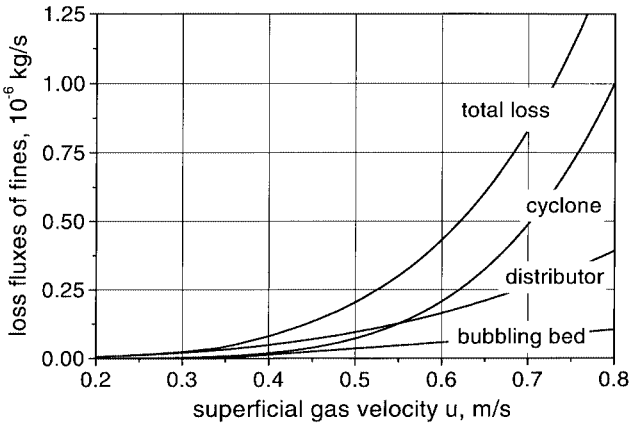

Figure 14. Influence of the superficial gas velocity on the extent of attrition in the individual regions and the overall fluidized-bed system.

Fluidized-bed facility from Figure 2, 97-G(fresh) catalyst, bed mass 5.5 kg.

Conclusions

The attrition-induced material loss of a fluidized-bed system is found to originate from various sources with quite different attrition mechanisms. In the present system grid, jet attrition, bubble-induced attrition, and cyclone attrition have been identified as the main attrition sources. The overall loss rate of the system can be described as the sum of these individual contributions, which have been modeled separately. The equations used for calculation take into account the design of the system, the operating conditions, and the material properties of the solids. The latter can be determined from attrition tests using for each source a particularly designed experimental setup that simulates the respective attrition stress.

From a comparison of jet and cyclone attrition tests with various catalyst materials, it has been found that the different attrition mechanisms in the individual regions do not allow conclusions to be drawn from a material's attrition characteristics with respect to one attrition source as opposed to another source. Even the ranking of different materials with respect to their attrition resistance cannot be transferred from one source to another. Hence, the individual attrition sources for each material must be studied in isolation in order to obtain the respective attrition characteristics.

The simulation of the fluidized-bed system revealed that the relative contributions of the individual sources to the system's total attrition-induced loss rate are different for different fluidizing velocities. At smaller superficial velocities the perforated-plate distributor turns out to be the main attrition source, though after exceeding a critical gas velocity, the cyclone attrition becomes predominant, which can be mainly attributed to the entrainment from the bed. With increasing gas velocity the entrainment rate increases, as does the material mass that is subjected to cyclone attrition per unit time. Furthermore, the material that enters the cyclone becomes coarser as the gas velocity increases, which also increases the extent of the cyclone attrition. Hence, taking the entrainment phenomenon into account, the cyclone attrition is most significantly affected by a change in the gas velocity.

In order to obtain an *a priori* modeling of the attrition-induced loss rate from the whole system, a description of both attrition rates caused by the individual sources and the effects of the entrainment is included in the present model, which can now be used to find the main attrition source in order to minimize the overall extent of attrition, or to estimate the effects of changes in the operating conditions of a given system. Furthermore, this procedure can be applied in the design of a new process in order to find the optimum combination of system design and operating conditions with respect to attrition.

Notation

A_t = cross-sectional area of the fluidized bed column, m^2
d_p = mean surface diameter, m
$d_{pc}(u)$ = mean surface diameter of the elutriated material defined by Eq. 20, m
K_b = rate constant of bubble-induced attrition defined by Eq. 10, $m^{-1} \cdot kg^{-n}$
$\dot{m}_f$ = mass flow of the fluid, kg/s
u_{mf} = minimum fluidization velocity, m/s

Literature Cited

Blinichev, V. N., V. V. Streltsov, and E. S. Lebedeva, "An Investigation of the Size Reduction of Granular Materials during their Processing in Fluidized Beds," *Int. Chem. Eng.*, **8**, 615 (1968).

Braca, R. M., and A. A. Fried, "Operation of Fluidization Processes," *Fluidization*, D. F. Othmer, ed., Reinhold, New York, p. 117 (1956).

de Vries, R. J., W. P. M. van Swaaij, C. Mantovani, and A. Heijkoop, "Design Criteria and Performance of the Commercial Reactor for the Shell Chlorine Process," *Proc. Euro. Symp. on Chem. React. Eng.*, Amsterdam, The Netherlands, B9-59 (1972).

Forsythe, W. L., and W. R. Hertwig, "Attrition Characteristics of Fluid Cracking Catalysts," *Ind. Eng. Chem.*, **41**, 1200 (1949).

Geldart, D., *Gas Fluidization Technology*, Wiley, Chichester, U.K. (1986).

Ghadiri, M., J. A. S. Cleaver, and V. G. Tuponogov, "Modelling Attrition Rates in the Jetting Region of a Fluidized Bed," *Proc. Symp. on Attrition and Wear in Powder Technology*, Utrecht, The Netherlands, p. 79 (1992).

Gwyn, J. E., "On the Particle-Size Distribution Function and the Attrition of Cracking Catalysts," *AIChE J.*, **15**, 35 (1969).

Kraft, W. W., W. Ullrich, and W. O'Connor, "The Significance of Details in Fluid Catalytic Cracking Units: Engineering Design, Instrumentation and Operation," *Fluidization*, D. F. Othmer, ed., Reinhold, New York, p. 184 (1956).

Patel, K., A. W. Nienow, and I. P. Milne, "Attrition of Urea in a Gas-Fluidised Bed," *Powder Technol.*, **47**, 257 (1986).

Pell, M., and S. P. Jordan, "Effects of Fines and Velocity on Fluid Bed Reactor Performance," *AIChE Symp. Ser.*, **84**(262), 68 (1988).

Pell, M., "Gas Fluidization," *Handbook of Powder Technology*, Vol. 8, Elsevier, Amsterdam, p. 97 (1990).

Reppenhagen, J., and J. Werther, "Particle Attrition Influences Cyclone Performance," *Preprints Euro. Symp. on Separation of Particles from Gases*, Nürnberg Messe GmbH, Nürnberg, Germany, p. 63 (1998a).

Reppenhagen, J., and J. Werther, "Catalyst Attrition in Cyclones," *Preprints Int. Particle Technol.*, Institution of Chemical Engineers, Rugby, UK (1998b).

Reppenhagen, J., and J. Werther, "Catalyst Attrition in Reactor Systems—Identification of Sources and Prediction of Effects," Canadian Chemical Engineering Conf., London, Ont., Canada (1998c).

Seville, J. P. K., M. A. Mullier, and M. J. Adams, "Attrition of Agglomerates in Fluidized Beds," *Proc. Eng. Found. Conf. on Fluidization*, Brisbane, Australia, p. 587 (1992).

Tasirin, S. M., and D. Geldart, "Entrainment of FCC from Fluidized Beds—A New Correlation for the Elutriation Rate Constants," *Powder Technol.*, **95**, 240 (1998) .

Trefz, M., and E. Muschelknautz, "Extended Cyclone Theory for Gas Flows with High Solids Concentration," *Chem. Eng. Technol.*, **16**, 153 (1993).

Vaux, W. G., and D. L. Keairns, "Particle Attrition in Fluid-Bed Processes," *Fluidization III*, J. R. Grace and J. M. Matsen, eds., Henniker, New York, p. 437 (1980).

Weeks, S. A., and P. Dumbill, "Method Speeds FCC Catalyst Attrition Resistance Determinations," *Oil Gas J.*, **88**, 38 (1990).

Werther, J., and J. Reppenhagen, "Attrition in Fluidized Beds and Pneumatic Conveying Lines," *Selected Topics on Fluidization, Solids Handling and Processing*, Noyes, Park Ridge, NJ (1999).

Werther, J., and W. Xi, "Jet Attrition of Catalyst Particles in Gas Fluidized Beds," *Powder Technol.*, **76**, 15 (1993).

Xi, W., "Katalysatorabrieb in Wirbelschichtreaktoren," PhD Thesis, Technical Univ., Hamburg-Harburg, Hamburg, Germany (1993).

Zenz, F. A., "Find Attrition in Fluid Beds," *Hydrocarbon Processing*, 103 (1971).

Zenz, F. A., and E. G. Kelleher, "Studies of Attrition Rates in Fluid-Particle Systems via Free Fall, Grid Jets, and Cyclone Impact," *J. Powder & Bulk Technol.*, **4**, 13 (1980).

Manuscript received Feb. 2, 1999, and revision received June 8, 1999.